preprint to be published in Adv.Mater. (2011)

Simulation of vapor-phase deposition and growth of a pentacene thin film on C_{60} (001)

Luca Muccioli*, Gabriele D'Avino and Claudio Zannoni

Dipartimento di Chimica Fisica e Inorganica and INSTM, University of Bologna, viale Risorgimento 4, IT-40136 Bologna, Italy.

* e-mail: Luca.Muccioli@unibo.it

Current research in organic electronics is clearly evidencing that the strive to produce efficient organic electronic devices requires high performance materials that can only be realized through a rational design [Special11]. Although polymer-based systems are at the moment the most appealing for market applications, mainly because of their solution processability, small molecule-based devices possess potential for commercialization, presenting comparable performances and a better batch-to-batch reproducibility of their properties [Walker11]. The interest in small molecules of well defined crystalline structure arises also from the fine control over final morphologies that can be achieved through vapour-phase growth techniques [Ruiz04, Rolin10], control that allows, with respect to polymer devices, a deeper understanding of the structure-electronic properties relationships. Indeed building an efficient electronic device (e. g. a solar cell) coincides to a large extent with the fine tuning of the electronic properties at the different interfaces, typically metal-organic, inorganic-organic, and organic-organic. In this communication we focus on the latter interface between two of the most studied *p*- and *n*-type molecular organic semiconductors, pentacene (A5) and C_{60} fullerene. These materials have been recently employed in producing rather efficient thin film bilayer solar cells [Yoo04, Mayer04, Yoo07, Cheyns07, Dissanayake07], ambipolar field effect transistors [Kuwahara04, Yan09, Cosseddu10] and low-voltage-operating organic complementary inverters [Na09].

The relative simplicity and the good performances of C_{60}/A5 heterojunctions has stimulated theoretical research on the electronic processes occurring at the interface: density functional theory [Yi09], valence-bond Hartree-Fock [Linares10] and microelectrostatic calculations [Verlaak09] have been employed in studying model interfaces of increasing complexity. These studies coherently underline the importance of relative molecular orientations and positions in determining the interface dipole and electronic couplings, i.e. the key factors governing exciton transport and fission, charge generation and separation [Rao10]. This in turn means that improving computational predictions of the molecular organization at the interface is fundamental to understanding experimental systems of great interest. This task can in principle be tackled by using classical atomistic force fields, but it is definitely not a straightforward one. Indeed, it has been recently recognized that molecular organizations at the interface depend on the preparation process and not just on thermodynamic state of the system, so that imitating the experimental preparation techniques is often necessary to produce realistic morphologies [Liu08, Cheung08, MacKenzie10, Clancy11, Beljonne11].

For this specific system, Clancy and co-workers applied classical simulations at both coarse-grained [Choudhary06] and atomistic detail [Goose07] to study some aspects of the pentacene growth on inert substrates and of the diffusivity of C_{60} on pentacene [Cantrell08]. In the following, we wish to investigate the growth of A5 on C_{60} with the aim of understanding the mechanism of the thin film formation and of identifying the most stable arrangement of pentacene on the C_{60} (001) surface as deposition proceeds. To do this we propose to mimic, by means of atomistic molecular dynamics simulations, the

vapour-phase deposition process by landing one A5 molecule at a time on a two-dimensional (2D) periodic C_{60} surface. This computational technique allows following step after step the non-equilibrium process of the adlayer formation on the substrate.

We find that initially A5 molecules lay flat on the C_{60} surface and diffuse quite rapidly, helped by the rotation of the supporting buckyballs [Luengo97]. This behaviour rapidly disappears as a few A5 molecules have been deposited, since they tend to aggregate in small clusters of about 10 molecules, causing a drop of the in-plane diffusivity. The clusters grow steadily and coalesce into a uniform film of almost horizontal A5 molecules, as shown in the snapshot in figure 1 at 0.54 monolayer (ML; coverage/thickness is given in units of completed ML of standing A5, 1ML corresponds to 112 molecules). In this film A5 molecules present a tendency to align parallel to each other locally, but without evidences of long-range order or herringbone packing. This trend persists until the coverage reaches about 0.6 ML. At higher coverage a collective reorientation takes place, with A5 molecules changing their orientation with respect to the surface from an almost planar to a roughly perpendicular alignment (see figure 1, 0.71-0.89 ML); the reorientation is associated with the onset of the herringbone packing.

By continuing the deposition we observe the partial completion of the first ML (ML1) and the concurrent formation of new aggregates of a few A5 molecules, laying flat on ML1 surface. Incoming A5 molecules easily diffuse on the ML1 surface until they find a vacancy to fill (see also additional snapshots at Supporting Information). Once all the lattice sites are filled, the flat aggregates grow in size, until again a striking collective reorientation takes place, similarly to what happens during the growth of ML1 (figure 1, 1.34-1.43 ML). After that A5 molecules in ML2 stand up, the herringbone packing sets in as observed in ML1. When ML2 is almost completed, we registered again a regime with flat-lying molecules translating on the surface in search of vacancies to fill.
The growth mechanism is quite similar in ML1 and ML2, as emerging from the plots of the film height and of the average tilt angle as a function of the coverage in figure 1: *i)* at low coverage the nucleation and growth of flat aggregates determines a steady increase of the film height; *ii)* at a critical coverage the molecules in the aggregate stand up and orient at about 55 degrees with respect to the substrate plane *iii)* new A5 molecules fill the vacancies in the layer and the height stays constant until ML completion. However it is worth noticing that the collective reorientation of A5 occurs at lower coverage in ML2 than in ML1.

The molecular organization on a given substrate is the result of the interplay between interactions among molecules in the adlayer and interactions between adlayer and substrate [DellaValle09, Djuric11]. To gain insights of the driving force of this spontaneous reorientation of A5 films and to understand why it happens at lower coverage for ML1 than for ML2, we calculated the relevant interaction energies among A5 admolecules and between admolecules and substrate (for ML2 the substrate is constituted by A5 molecules of ML1).
Interaction energies per admolecule as a function of the coverage are shown in figure 2. Despite the noise in the data, it is clear that, both in ML1 and in ML2, upon increasing the coverage the intra-adlayer energy (black circles) decreases at expenses of the adlayer-substrate energy (blue squares), driving the collective reorientation that occurs with a sudden drop in the intra-adlayer and total (red triangles) energy. In other words at low coverage the adlayer-substrate interaction dominates, keeping A5 molecules parallel to the substrate, but at high coverage molecules rearrange assuming a standing orientation in order to minimize intra-adlayer energy. The discontinuity in the system energy, occurring in concomitance with the molecular reorientation and with the establishment of the

herringbone packing of A5, can be considered as a signature of a 2D crystallization. The difference between the critical coverage at which the reorientation transition occurs in the two ML, can be traced back to the adhesion energy between one lying A5 molecule on the C_{60} (001) surface and on ML1: this energy is about 3 kcal/mol larger for the C_{60} substrate, causing the collective reorientation to occur at higher coverage.

After the deposition of two complete MLs, the sample was equilibrated at 300 K and the 2D crystalline order was characterized by calculating the diffraction pattern of each ML. The 2D representation of ML1 and its diffraction pattern are shown in the left and right panels of figure 3, respectively. The unit cell obtained from the most intense diffraction spots, shown as a red frame in figure 3, contains two A5 molecules (Z=2). Cell parameters measured for the two ML are identical and are given in table 1 [Note1]. The cell predicted by our simulation can be directly compared to the experimental unit cells; while simulated values of ***a*** and γ are very close to experimental ones, the cell parameter ***b*** is rather different. Such a discrepancy is due to the inclination of A5 molecules, and can be quantified by the spacing between the ML, ***d***(001). Our simulation leads to ***d***(001)=12.8 Å, a value lower than the typical values reported for A5 bulk and thin film polymorphs on SiO_2, but in good agreement with the spacing of 12 ± 2 Å reported by Dougherty et al. for A5 grown on C_{60}/Ag(111) [Dougherty09]. An interesting feature of the simulated interface is the relative orientation of substrate and adlayer lattices, leading to the alignment of A5 centers of mass of ML1 along the C_{60} [1-10] direction (blue line in left panel of figure 3) [Note2].

Further experimental confirmations of our results can be found in the recent literature [Hu05, Al-Mahboob09, Duhm09, Liu09]: Hu et al deposited A5 on a C_{60}-terminated self-assembled monolayer on Au, finding that, differently from what happens on the bare metal, A5 grows with the long axis almost perpendicular to the surface [Hu05]. Al-Mahboob ***et al.*** studied the temperature dependence of growth of A5 on C_{60} (111) by means of low energy electron microscopy, noting two distinct types of nucleation: an earlier nucleation of a lying-down crystalline phase (not observed here) and a delayed nucleation of a standing-up phase, the latter becoming favorite above 400 K [Al-Mahboob09]. The standing up phase was also detected at room temperature with scanning tunneling microscopy in islands of A5 grown on C_{60} /Ag(111) [Dougherty09]. Finally, both Koch's [Duhm09] and Fahlman's group [Liu09] reported coverage-dependent changes in the ultraviolet photoelectron spectra of A5 when deposited on C_{60}/PEDOT:PSS and C_{60}/Au, respectively. In particular, in the second study it was shown that the X-ray absorption features of standing A5, develop at a nominal thickness of about 0.8 ML, in excellent agreement with the critical coverage for lying to standing orientation predicted by our simulation.

Concluding, we found that the growth of ML of A5 on C_{60} (001) proceeds in two coverage-dependent steps: in the first, A5 molecules lay flat and disordered on the C_{60} surface, with a steady growth of the film height. In the second, A5 molecules reorient perpendicular to the surface and self-assemble in a crystalline packing. This mechanism is governed by the fact that at a high coverage the energetically favored arrangement of A5 on C_{60} (001) is a layer of standing molecules, matching the necessary conditions for a layer-by-layer (Frank-van der Merwe) growth [Choudary06] and leading to a highly ordered molecular film. We believe that this study represents a promising and significant progress towards the use of atomistic simulations in studying the complex out-of-equilibrium irreversible process of organic crystal growth.

Experimental Section

Both compounds are described with AMBER force field [Cornell95], for which we tested

the capability of reproducing the cell parameters at 300 K and p=1 atm starting from the experimental crystallographic geometries. For A5 we rely on the results in reference [Martinelli09], while for C_{60} a 4x4x4 supercell yielded to a cell parameter *a*=14.048 Å, to be compared with the experimental value at room temperature of 14.152 Å [Andre92]. In addition the orientational order-disorder transition of C_{60} at 260 K [Allemand91] and the temperature dependence of the cell parameter [Chang06] are correctly reproduced. The agreement between experiments and simulation ensures that the force field provides a sensible description of the intermolecular forces.

Molecular dynamics simulation of the deposition was performed with the Orac code [Procacci97] in the NVT ensemble at T=500 K, using a velocity scaling thermostat and timestep 1 ns. The relatively high temperature was chosen as it is beneficial for accelerating the molecular motion without changing significantly the free energy landscape (both compounds sublimates at higher temperatures, ~645 K for A5, ~620 K for C_{60}). The C_{60}(001) surface was prepared as a 4x4x2 supercell [Liu91], composed of 128 molecules. The simulation box was enlarged in the z direction, creating an empty region where A5 can be deposited, obtaining a final box size of 56.2 x 56.2 x 200 Å. Periodic boundary conditions are imposed in the three dimensions, but because of the large empty space along z, they are effective only in 2D.

The vapour deposition of A5 was mimicked by inserting into the box one A5 molecule every 250 ps. This frequency corresponds to an unrealistically high flux rate (≈0.1 molecules $nm^{-2}ns^{-1}$ and corresponding to $0.5 \cdot 10^9$ Å/s for a standing up film), necessary to make the simulation feasible, but that may kinetically favor the growth of amorphous films [Ruiz04, Choudhary06]. Each new molecule had random position (within 10 Å from the interface) and velocity, but the same geometry and orientation (at about 15 degrees with respect to the surface). Desorption occurred rarely and only for newly inserted A5 molecules; when this happened, the desorbed A5 was removed from the box and a new A5 was inserted as explained above.

The scheme was repeated for 224 molecules, corresponding to two complete A5 ML, and to a total simulation time of 60 ns. After completing the deposition, the sample was equilibrated at 300 K for 5 ns. 2D representations of the monolayers were obtained by drawing each molecule as an ellipse with semiaxes aligned with the short A5 axes and with center coinciding with the A5 center of mass. A5 positions and orientations were averaged over 1 ns of the equilibrated trajectory at 300 K. The 2D representation of A5 molecules is a function that has value 1 within ellipses contours and 0 outside. The main features of the diffraction pattern does not depend on the specific values of the ellipse semi-axes (a=2.5 Å, b=0.3 Å are used here). Diffraction patterns were calculated as squared Fourier transforms of the real space 2D representations with the Octave numerical computation suite.

Acknowledgements
The research leading to these results has received funding from the European Community's Sixth Framework Programme (FP6/2002-2006) under the project MODECOM, and from FP7 (2007-2013) under grant agreement n° 212311 of the ONE-P project, and grant agreement n° 228424-2 of the MINOTOR project.
We are grateful to Prof. Aldo Brillante, Prof. Guido Raffaele Della Valle and Dr. Elisabetta Venuti (University of Bologna) for helpful discussions regarding A5 crystal structures and their characterization.

Bibliography

[Allemand91] P. M. Allemand, G. Srdanov, A. Koch, K. Khemani, F. Wudl, Y. Rubin, F. Diederich, M. M. Alvarez, S. J. Anz, R. L. Whetten, *"The unusual electron spin resonance of fullerene C_{60} anion radical"*, J. Am. Chem. Soc. 1991, 113, 2780.

[Al-Mahboob09]A. Al-Mahboob, J.T. Sadowski , Y. Fujikawa, T. Sakurai, *"The growth mechanism of pentacene-fullerene heteroepitaxial films"*, Surf. Sci. 2009, 603, L53.

[Andre92] D. Andre, A. Dworkin, H. Szwarc, R. Ceolin, V. Agafonov, C. Fabre, A. Rassat, L. Straver, P. Bernier, A. Zahab, *"Molecular packing of fullerene C-60 at room-temperature"*, Mol. Phys. 1992, 76, 1311.

[Beljonne11] D. Beljonne, J. Cornil, L. Muccioli, C. Zannoni, J.-L. Brédas, F. Castet *"Electronic Processes at Organic-Organic Interfaces: Insight from Modeling and Implications for Opto-Electronic Devices"* Chem. Mater., 2011, 23, 591.

[Campbell61] R. B. Campbell, J. M. Robertson, J. Trotter, *"The crystal and molecular structure of pentacene"*, Acta Cryst. 1961, 14, 705.

[Cantrell08] R. Cantrell, P. Clancy, "*A computational study of surface diffusion of C-$_{60}$ on pentacene"* Surf. Science 2008, 602, 3499.

[Chang06] J. Chang, S. I. Sandler, *"Free energy of the solid C_{60} fullerene orientational order-disorder transition"*, J. Chem. Phys. 2006, 125, 054705.

[Cheyns07] D. Cheyns, H. Gommans, M. Odijk, J. Poortmans, P. Heremans, *"Stacked organic solar cells based on pentacene and C_{60}"*, Solar Energy Materials & Solar Cells 2007, 91, 399.

[Cheung08] D. L. Cheung, A. Troisi, *"Modelling charge transport in organic semiconductors: from quantum dynamics to soft matter"*, Phys. Chem. Chem. Phys 2008, 10, 5941.

[Choudhary06] D. Choudhary, P. Clancy, R. Shetty, F. Escobedo, *"A Computational Study of the Sub-monolayer Growth of Pentacene"*, Adv. Funct. Mater. 2006, 16, 1768.

[Clancy11] P. Clancy, *"Application of Molecular Simulation Techniques to the Study of Factors Affecting the Thin-Film Morphology of Small-Molecule Organic Semiconductors"* Chem. Mater., 2011, 23, 522.

[Cornell95] W. D. Cornell, P. Cieplak, C. I. Bayly, I. R. Gould, K. M. Merz Jr., D. M. Ferguson, D. C. Spellmeyer, T. Fox, J. W. Caldwell, P. A. Kollman, *"A Second Generation Force Field for the Simulation of Proteins, Nucleic Acids, and Organic Molecules"*. J. Am. Chem. Soc. 1995, 117, 5179.

[Cosseddu10] P. Cosseddu, A. Bonfiglio *"Influence of device geometry in the electrical behavior of all organic ambipolar field effect transistors",* Appl. Phys. Lett. 2010, 97, 203305.

[DellaValle09] R. G. Della Valle, E. Venuti, A. Brillante, A. Girlando*, "Molecular Dynamics Simulations for a Pentacene Monolayer on Amorphous Silica"*, ChemPhysChem 2009, 10, 1783.

[Djuric11] T. Djuric,T. Ules,H.-G. Flesch, H. Plank, Q. Shen, C. Teichert, R. Resel, M. G. Ramsey, *"Epitaxially Grown Films of Standing and Lying Pentacene Molecules on Cu(110) Surfaces",* Cryst. Growth Des. 2011, 11, 1015.

[Dougherty09] D. B. Dougherty, W. Jin, W. G. Cullen, J. E. Reutt-Robey, S. W. Robey, *"Striped domains at the pentacene:C-60 interface",* Appl. Phys. Lett. 2009, 94, 023103.

[Duhm09] S. Duhm, I. Salzmann, R. L. Johnson, N. Koch, "Electronic non-equilibrium conditions at C_{60}–pentacene heterostructures", J. Electr. Spectr. Rel. Phen. 2009, 174, 40.

[Goose07] J. E. Goose, P. Clancy, *"Exploring the Energetic Deposition of Pentacene on Pentacene through Molecular Dynamics Simulations"*, J. Phys. Chem. C 2007, 111, 15653.

[Kuwahara04] E. Kuwahara, Y. Kubozono, T. Hosokawa, T. Nagano, K. Masunari, A. Fujiwara *"Fabrication of ambipolar field-effect transistor device with heterostructure of C_{60} and pentacene"* Appl. Phys. Lett. 2004, 85, 4765.

[Liu91] S. Z. Liu, Y. J. Lu , M. M. Kappes, J. A. Ibers. *"The structure of the C_{60} molecule - X-ray crystal-structure determination of a twin at 110-K"*, Science, 1991, 254,408.

[Liu08] H. Liu, Z. Lin, L. V. Zhigilei, P. Reinke, *"Fractal Structures in Fullerene Layers: Simulation of the Growth Process"*, J. Phys. Chem. C 2008, 112, 4687.

[Liu09] X. Liu, Y. Zhan, S. Braun, F. Li, and M. Fahlman, "*Interfacial electronic properties of pentacene tuned by a molecular monolayer of C-60"*, Phys. Rev. B. 2009, 80, 115401.

[Luengo97] G. Luengo, S. E. Campbell, V. I. Srdanov, F. Wudl, and J. N. Israelachvili, *"Direct Measurement of the Adhesion and Friction of Smooth C_{60} Surfaces"*, Chem. Mater. 1997, 9, 1166.

[MacKenzie10] R. C. I. MacKenzie, J. M. Frost, and J. Nelson, *"A numerical study of mobility in thin films of fullerene derivatives"*, J. Chem. Phys. 2010, 132, 064904.

[Martinelli09] N. G. Martinelli, M. Savini, L. Muccioli, Y. Olivier, F. Castet, C. Zannoni, D. Beljonne, J. Cornil, *"Modeling Polymer Dielectrics/Pentacene Interfaces: On the Role of Electrostatic Energy Disorder on Charge Carrier Mobility"*, Adv. Funct. Mater., 2009, 19, 3254.

[Na09] J. H. Na, M. Kitamura, Y. Arakawa *"Low-voltage-operating organic complementary circuits based on pentacene and C_{60} transistors",* Thin Solid Films 2009, 517, 2079.

[Note1] In ML1 we found weaker diffraction spots corresponding to a Z=4 unit cell. The cell doubling is originated by the C_{60} surface: in fact two A5 molecules lean on top of the C_{60} [1-10] rows, while the other two molecules stick in between the rows. Simulations performed without enforcing periodic boundary conditions (pbc) produced the disappearance of the Z=4 feature in the diffraction pattern, that is therefore considered an artifact of pbc.

[Note 2] The relative orientation of the two lattices is a genuine effect that survives also in simulations with relaxed periodic boundary conditions, while the coincidence-II epitaxy between the A5 and C_{60} lattices that is observed here, is another artifact of pbc.

[Procacci97] P. Procacci, E. Paci, T. Darden, M. Marchi*, "ORAC: A Molecular Dynamics Program to Simulate Complex Molecular Systems with Realistic Electrostatic Interactions"*, J. Comput. Chem.,1997, 18, 1848.

[Rao10] A. Rao, M. W. B. Wilson, J. M. Hodgkiss, S. Albert-Seifried, H. Bässler, R. H. Friend, *"Exciton Fission and Charge Generation via Triplet Excitons in Pentacene/C_{60} Bilayers"*, J. Am. Chem. Soc. 2010, 132, 12698.

[Rolin10] C. Rolin , K. Vasseur, J. Genoe, P. Heremans, *"Growth of pentacene thin films by in-line organic vapor phase deposition"* Org. Electron. 2010, 11, 100.

[Ruiz04] R. Ruiz, D. Choudhary, B. Nickel, T. Toccoli, K.-C. Chang,A. C. Mayer, P. Clancy, J. M. Blakely, R. L. Headrick, S. Iannotta, G. G. Malliaras, "*Pentacene Thin Film Growth*", Chem. Mater. 2004, 16, 4497.

[Schiefer07] S. Schiefer, M. Huth, A. Dobrinevski, B. Nickel "*Determination of the Crystal Structure of Substrate-Induced Pentacene Polymorphs in Fiber Structured Thin Films"* J. Am. Chem. Soc. 2007, 129, 10316.

[Siegrist01] T. Siegrist, C. Kloc, J. H. Schön, B. Batlogg, R. C. Haddon, S. Berg, G. A. Thomas *"Enhanced Physical Properties in a Pentacene Polymorph"* Angew. Chem. Int. Ed. 2001, 40, 1732.

[Special11] see Chemistry of Materials *"Special Issue on π-Functional Materials"*, 2011, 23.

[Verlaak09] S. Verlaak, D. Beljonne, D. Cheyns, C. Rolin, M. Linares, F. Castet, J. Cornil, P. Heremans, "*Electronic Structure and Geminate Pair Energetics at Organic-Organic Interfaces: The Case of Pentacene/C-60 Heterojunctions"* Adv. Funct. Mater. 2009, 19, 3809.

[Walker11] B. Walker, C. Kim, T.-Q. Nguyen, "*Small Molecule Solution-Processed Bulk Heterojunction Solar Cells*" Chem. Mater., 2011, 23, 470.

[Yan09] H. Yan, T. Kagata, H. Okuzaki, *"Ambipolar pentacene/C_{60}-based field-effect transistors with high hole and electron mobilities in ambient atmosphere"*, Appl. Phys. Lett. 2009, 94, 023305.

[Yi09] Y. Yi, V. Coropceanu, J.-Luc Brédas *"Exciton-Dissociation and Charge-Recombination Processes in Pentacene/C_{60} Solar Cells: Theoretical Insight into the Impact of Interface Geometry"* J. Am. Chem. Soc. 2009, 131, 15777.

[Yoo04] S. Yoo S, B. Domercq and B. Kippelen, *"Efficient thin-film organic solar cells based on pentacene/C_{60} heterojunctions"*, Appl. Phys. Lett. 2004, 85, 5427.

[Yoo07] S. Yoo, W. J. Potscavage Jr., B. Domercq, S.-H. Han, T.-D. Li, S. C. Jones, R. Szoszkiewicz, D. Levi, E. Riedo, S. R. Marder, B. Kippelen, "*Analysis of improved photovoltaic properties of pentacene/C_{60} organic solar cells: Effects of exciton blocking layer thickness and thermal annealing"*, Solid-State Electron. 51 (2007) 1367–1375

Figures and Tables

Table 1: In plane lattice experimental and calculated cell parameters for pentacene polymorphs.

System	*a* (Å)	*b* (Å)	γ (º)	*d(001)* (Å)
exp (thin film) [Schiefer07]	5.958	7.596	89.80	15.4
exp (solution) [Campbell61]	6.06	7.90	85.8	14.5
exp (vapour) [Siegrist01]	6.253	7.786	84.61	14.1
exp on C_{60} (111) [Al-Mahboob09]	5.9	7.6	88	-
ML1-ML2 on C_{60} (001)	6.1	9.3	86	12.8

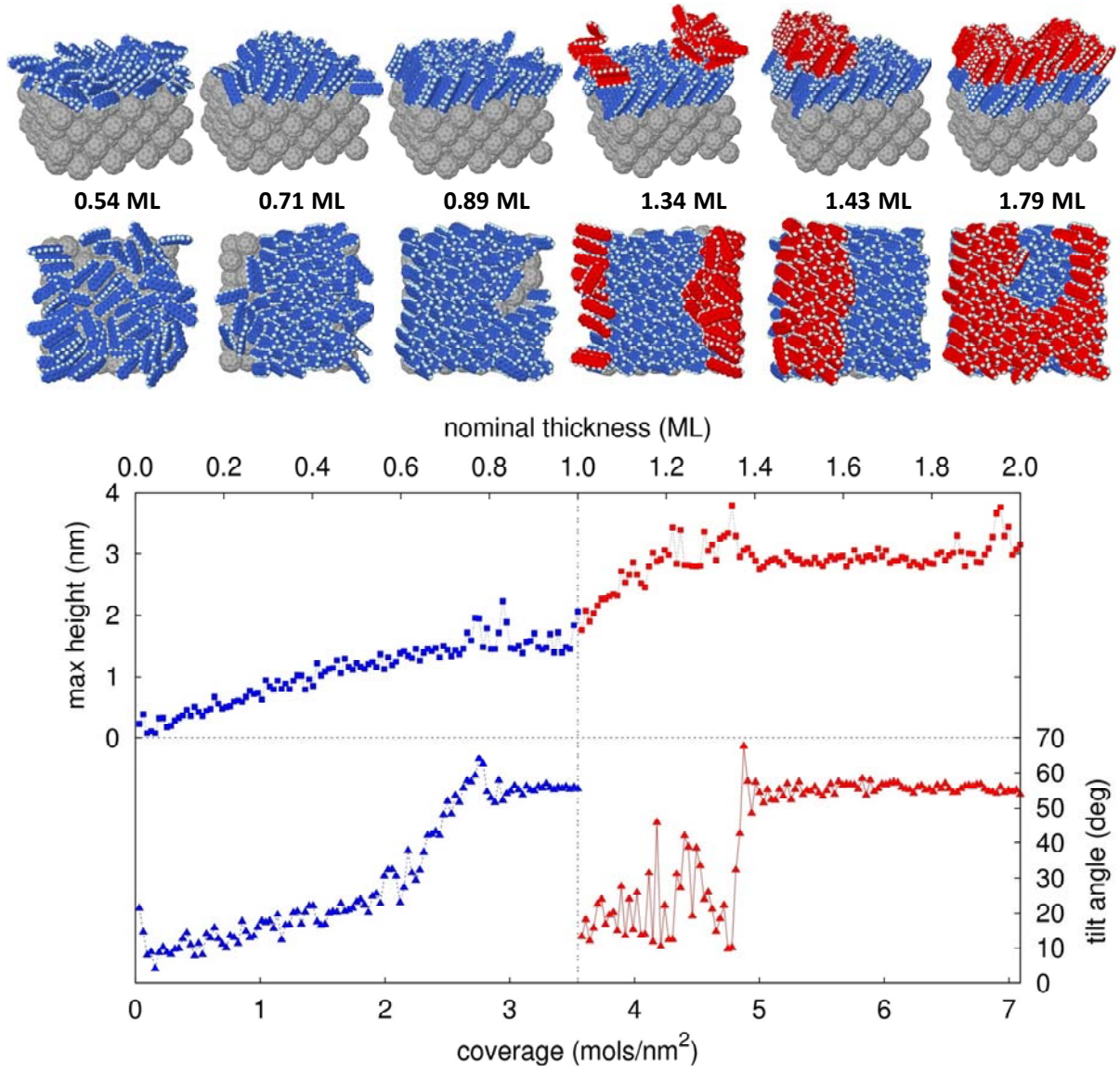

Figure 1: Top: Selected simulation snapshots showing the transition from planar to perpendicular alignment for the first (blue) and second (red) monolayer. Bottom: Maximum film height and tilt angle (formed by A5 long axis and C_{60} surface) measured during the growth of ML1 and ML2. Two regimes are recognized: at low coverage, A5 molecules lay flat on the C_{60} surface, leading to a steady growth of the film height. When coverage reaches a critical value (~0.6 for ML1 and ~1.4 for ML2), reorganization occurs and A5 molecules orient their long axis at about 55 degree with respect to the surface plane. The height and the angle remain constant until completion of the ML.

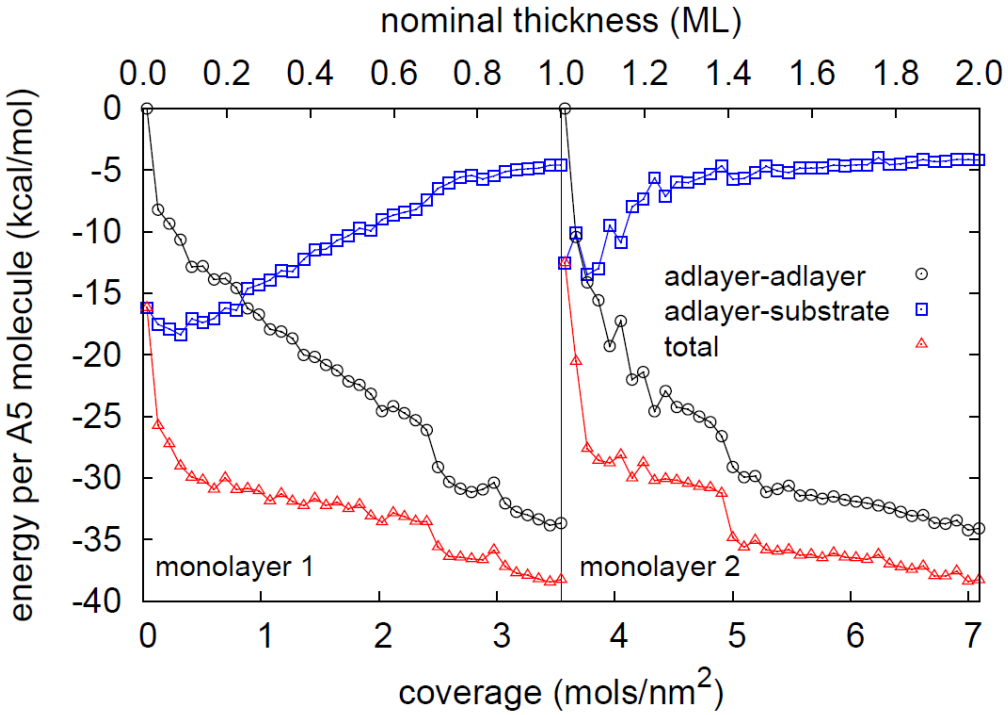

Figure 2: Intermolecular interaction energies in the growth of the first and second A5 ML on C_{60}, averaged over the last 50 ps of each deposition step: Interaction of A5 adlayer with the substrate (blue squares), intra-adlayer interactions (black circles), and total interaction (red lines). A sharp decrease of the total energy per molecule, associated to the flat-to-standing reorientation, is observed at coverages of ~0.7 and ~1.4 ML.

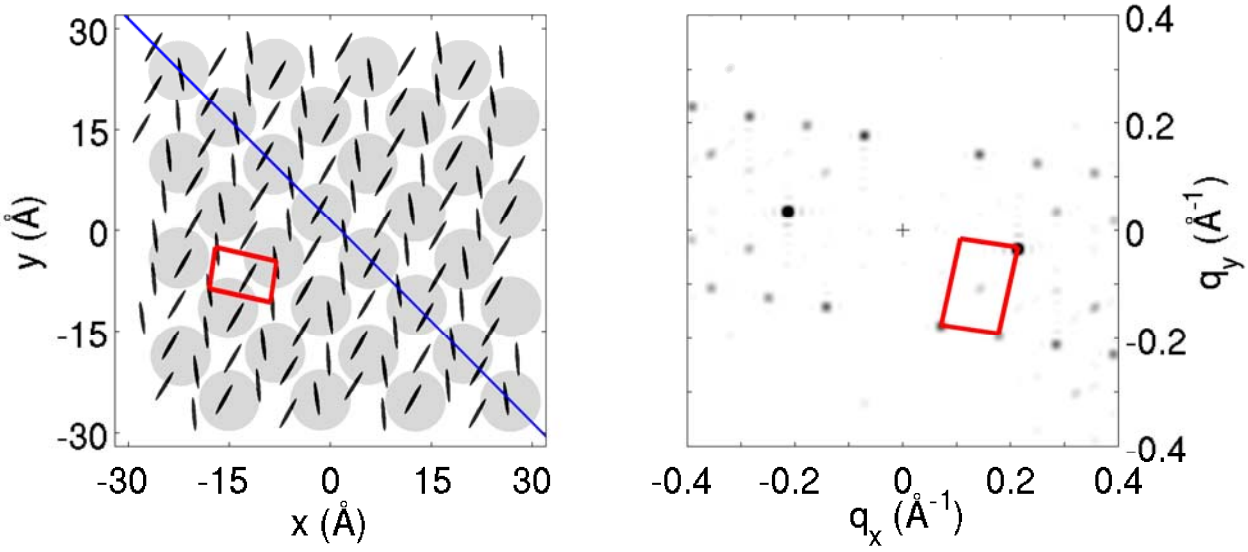

Figure 3: Left panel: schematic drawing of the first A5 ML (black ellipses) and of the upper layer of the C_{60} (001) surface (gray circles); the red frame shows the Z=2 unit cell of the A5 lattice, the blue line marks the [1-10] direction of the C_{60} surface. Right panel: 2D diffraction pattern of A5 ML1; the red frame shows the unit cell in the reciprocal lattice.